https://doi.org/10.5194/egusphere-2026-5413
Preprint. Discussion started: 21 September 2026

Regional spectral decay model for the Sichuan, China: Application in ground motion simulation of the Ms 6.0 Changning earthquake

Pengfei Dang[1], Bingyan Zhao[1], Qifang Liu[2], Jie Cui[3], Xinjian Jia[4]

[1] School of Civil Engineering and Future Cities, Ningbo University, Ningbo, China.

[2] School of Civil Engineering, Suzhou University of Science and Technology, Suzhou, China.

[3] School of Civil Engineering and Transportation, Guangzhou University, Guangzhou, China.

[4] Hebei Zhenchuang Electronic Technology Co., Ltd, Langfang, China.

Corresponding author: Pengfei Dang (dangpengfei@nbu.edu.cn)

Author affiliations

Pengfei Dang (dangpengfei@nbu.edu.cn)

Address:

School of Civil Engineering and Future Cities, Ningbo University, Ningbo, China.

No.818 Fenghua Road,

Jiangbei District, 315211, Ningbo, Zhejiang, China

ORCID: 0000-0001-6780-6453

Bingyan Zhao (bingyan2026@163.com)

Address:

School of Civil Engineering and Future Cities, Ningbo University, Ningbo, China.

No.818 Fenghua Road,

Jiangbei District, 315211, Ningbo, Zhejiang, China

https://doi.org/10.5194/egusphere-2026-5413
Preprint. Discussion started: 21 September 2026

Qifang Liu (iemliu@126.com)

Address:

School of Civil Engineering, Suzhou University of Science and Technology, Suzhou, China.

No. 1707 Binhe Road,

Huqiu District, 215011, Suzhou, Jiangsu, China

Jie Cui (jcui2009@qq.com)

Address:

School of Civil Engineering and Transportation, Guangzhou University,

No.230 Waihuan West Road,

Panyu District, 510006, Guangzhou, Guangdong, China

Xinjian Jia (756405086@qq.com)

Address:

School of Civil Engineering and Future Cities, Ningbo University, Ningbo, China.

No.36 Research Building, Tianshan International Entrepreneurship Base,

Yanjiao Economic and Technological Development Zone, 065201, Langfang, Hebei, China

https://doi.org/10.5194/egusphere-2026-5413
Preprint. Discussion started: 21 September 2026

Regional spectral decay model for the Sichuan, China: Application in ground motion simulation of the Ms 6.0 Changning earthquake

Abstract 4260 recordings of 165 events by 168 stations were used to calculate the spectral decay kappa parameter. The kappa values of the two horizontal components were similar and generally larger than those of the vertical component. The impact of magnitude and site condition on the κ_0 value was also investigated, which showed that κ_0 increased with magnitude, indicating that κ_0 is influenced by source effects. In addition, the results showed that softer sites have higher κ_0 values, indicating that site conditions significantly affect κ_0 estimates. The single-station κ_0 values showed little difference between the two horizontal components, both of which were significantly greater than the κ_0 value of the UD component. Furthermore, the relationships between κ_0 and Vs30 were derived, which indicates that κ_0 value decreases with increasing parameter Vs30. Moreover, the logκ_0-logf_0 correlations estimate the κ_0 better than the ln$V$s30-κ_0 correlation does. Finally, we performed ground motion simulations at 16 stations to validate the derived site-based kappa model. Ground motion simulations at 16 stations demonstrate that both site- and event-related κ_0 mainly affect high-frequency amplitudes. These findings provide a basis for seismic attenuation study and refined ground motion simulation in the study region.

1. Introduction

In recent years, seismic activity has been very frequent in the western-central Sichuan, China. Especially after the Mw7.9 Wenchuan earthquake in 2008, the intensity of seismic activity in the region significantly increased. (Zuo et al., 2021; Zhang et al., 2021) In the study area, many earthquake events with magnitudes of 1.0–7.0 have occurred. The most typical earthquake events are the Lushan 6.6-magnitude earthquake and the Jiuzhaigou 7.0-magnitude earthquake, which occurred in 2013 and 2017, respectively. These findings demonstrate that western-central Sichuan, China, especially the western and northwestern parts of the Sichuan Basin, are already in a relatively active state. The aftershock activity of the Changning 6.0-magnitude earthquake that occurred on June 17, 2019 (local time), was very strong, with only 4 aftershocks of magnitude 5 or above, reflecting the complex seismic activity background in the study area. The China Earthquake Network Center reported that the epicenter of the Changning event was located at 104.90°E and 28.34°N, with a depth of 16 km. Strong tremors were felt in Sichuan Province and its surrounding areas, such as Chongqing, Yunan, Guizhou, and many other regions. As of June 19, 2019, the Changning earthquake in Sichuan resulted in 13 deaths and 199 injuries, and approximately 1000000 people were affected, causing significant impacts on local society, production, and daily life (Guo et al., 2022). As Changning is located at the junction of Yunnan, Sichuan and Guizhou provinces, and geological structures are at the edge of the transition from the Yunna-Guizhou Plateau to the Sichuan Basin, the geological structure background is relatively complex. Changning was formed during multiple periods of interactions between the Qinghai-Tibet Plateau and the Sichuan Basin, with NE-trending structures, NW-trending structures, and even the superposition of two structures.

The spectral amplitude significantly decreases at high frequencies when the frequency exceeds a certain value (Anderson and Hough, 1984; Douglas et al., 2010). The spectral attenuation characteristics can be described as two types of filters: the kappa (κ) filter and the f_{max} filter. The κ filter is defined as $\exp(-\pi f \kappa)$ (Anderson and Hough, 1984; Huang et al., 2024), and the f_{max} filter is defined as $[1+(f/f_{max})^8]^{-1/2}$ (Hanks, 1982). The concept of kappa has been applied in many fields of earthquake engineering since its inception, such as site amplification (Campbell, 2013), ground motion prediction equations (Laurendeau et al., 2013; Bora et al., 2015), and stochastic

https://doi.org/10.5194/egusphere-2026-5413
Preprint. Discussion started: 21 September 2026

ground motion simulation (Motazedian, 2005; Dabaghi and Kiureghian, 2016). Research has shown that significant differences in ground motion are noted between earthquakes recorded at multiple stations and multiple earthquakes recorded at a single station (Neighbors et al., 2015). Although kappa (κ) is defined to describe the spectral decay at a station, there is still controversy over the main mechanism controlling high-frequency attenuation (Tsai and Chen, 2000; Purvance and Anderson, 2003; Douglas et al., 2010). Many studies have confirmed that kappa is related mainly to site effects (Hanks, 1982; Anderson and Hough, 1984; Rovelli et al., 1988; Anderson, 1991), whereas some studies have indicated that kappa is related to distance (Anderson, 1991; Castro et al., 2000;), earthquake magnitude, focal mechanisms, and focal depth (Papageorgiou and Aki, 1983; Purvance and Anderson, 2003; Parolai and Bindi, 2004), and some studies have indicated that kappa is related to source, path, and site effects (Tsai and Chen, 2000; Kilb et al., 2012). Although the physical meaning of kappa is still unknown, in the field of earthquake engineering, parameter κ is usually defined as a site-related parameter that is used to describe the effects of site conditions in ground motion simulations. Kappa can be divided into two parts, namely, κ_R and κ_0 (Anderson and Hough, 1984), where κ_0 (zero-distance κ_0) is the κ value at R = 0 and is used to define attenuation from the shallow subsurface at the site, and κ_R is related to distance and is used to describe the regional slope. Research has shown that zero-distance κ_0 is related to the Vs30 parameter, which is defined as the shear-wave velocity averaged over the top 30 m of soil, and κ_0 is smaller at rock sites and greater at soft soil sites (Silva et al., 1998; Ktenidou et al., 2014; Sertcelik et al., 2022).

In this study, we estimated the spectral decay kappa values using ground motion recordings observed in western-central Sichuan, China, and investigated the relationship between event-related kappa and epicentral distance. Then, we investigated the impact of different earthquake magnitudes and site conditions on kappa calculations. Furthermore, to assess how different estimation methods affect the value of zero-distance κ_0, this study adopts a fixed-slope model instead of the free-fitting approach widely used in previous studies. On the basis of a single station for which 4 or more records were recorded, the zero-distance κ_0 of a single station was estimated, and the relationships between κ_0-Vs30 and κ_0-f_0 were analyzed. Finally, the acceleration waveforms of 16 stations during the Ms 6.0 Changning earthquake in China were simulated using the stochastic finite fault method to examine the influence of the derived site-based kappa model on the simulation results. These findings provide a theoretical basis for the systematic study of the κ model in the western-central Sichuan, China.

2. Ground motion dataset

From 2007 to 2022, a total of 4260 three-component (e.g., east–west, EW; north–south, NS; up–down, UD) records of 165 earthquakes with magnitudes of 3.0–6.0 recorded by 168 stations in western-central Sichuan, China, were collected. These selected stations are distributed mainly in the western part of the Sichuan Basin, as shown in Figure 1. In this study, we excluded earthquakes with magnitudes less than 3.0 and earthquakes with magnitudes greater than 6.0. On the one hand, owing to the relatively high corner frequency of small earthquake events, this may affect the estimation of spectral decay kappa values. On the other hand, large-scale earthquake events may lead to the nonlinear behavior of local sites, which can result in deviation in kappa estimation (Askan et al., 2014). The recordings selected in this study were provided by the China Strong Motion Network Centre and the sampling frequency was 200 Hz. In this study, we converted the surface wave magnitude (Ms) to the local magnitude (M_L) using the relationship between them, which can be defined in the form of $M_s = 1.13 \times M_L - 1.08$ (Wang et al., 2010).

https://doi.org/10.5194/egusphere-2026-5413
Preprint. Discussion started: 21 September 2026

Before the Fourier amplitude spectrum (FAS) was calculated, each raw recording of three components was filtered by a Butterworth filter with a filtering range of 0.1–60 Hz after baseline correction. The *P* and *S*

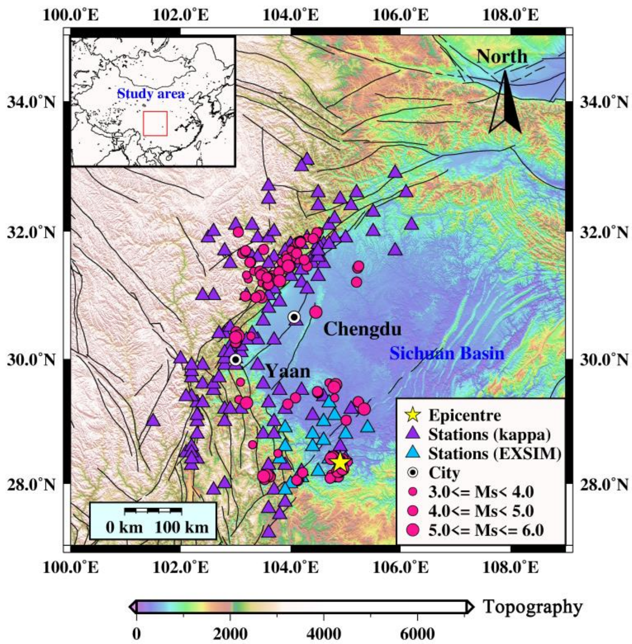

Figure 1. Distribution of selected stations and earthquakes, with purple triangles representing stations used for estimating spectral decay parameters, blue triangles representing stations used for ground motion simulation, a yellow pentagram representing the epicenter of the Changning earthquake in China, and red circles representing earthquake events (scaled by M_L) used for estimating spectral decay kappa. The inset map in the upper left corner shows the location of the study area on a map of China.

waves were picked using the vertical and horizontal components of ground motion, respectively, which was performed manually through a visual inspection of the acceleration waveforms. In this study, the record recorded by Station 015JYC was selected to demonstrate the step of extracting S waves:

①The starting and ending points of the S-wave were determined by the time when 5% of the energy was accumulated (Husid, 1967) and the time when the cumulative root-mean-square function obtained from the acceleration waveforms began to decrease over time (Hassani, 2015). The S-wave window length was limited to a maximum of 15 s to avoid contamination by coda waves (Moya *et al*., 2000; Drouet and Chevrot, 2008).

② A 10% Hanning taper was used on both time windows to eliminate truncation errors (Dang et al., 2024; Dang et al., 2025).

③ For each waveform, a noise window of the same length as the S-wave window was selected from the pre-event portion (Figure S1).

Notably, as long as the energy portion of the S-waves is extracted, the window length used has little effect on the estimation of kappa (Tsai and Chen, 2000; Douglas et al., 2010; Neighbors et al., 2015). Askan et al. (2014)

https://doi.org/10.5194/egusphere-2026-5413
Preprint. Discussion started: 21 September 2026

reported that smoothing the FAS is a necessary step for reliable estimation of the spectral decay kappa parameter. In our work, both the S-wave and noise windows were transformed to the frequency domain via fast Fourier transform. The FAS curves were then smoothed using the Konno and Ohmachi (1998) windowing function with a smoothing parameter *b* of 20 to avoid abrupt variations. In this case, records with a signal-to-noise ratio (SNR) greater than 3 were selected, and the smoothed FAS values can be obtained from the root mean square (RMS) of the two horizontal components to reduce the influence of the azimuthal direction (Pozo et al., 2023). Therefore, the RMS FAS of the two horizontal components and the FAS of the vertical component were used to calculate the H/V curve. After the above screening steps were completely, a total of 4260 acceleration time histories of three components from 165 small- and medium-sized earthquake events (3.0≤M≤6.0) recorded at 168 stations were selected (Figure 2). As shown in the figure, the epicentral distances are distributed within 250 km, with a depth of less than 30 km, and the data are evenly distributed within the epicentral distance and depth range. In addition, the detailed information of the selected stations is summarized in Table S1. To ensure the reliability of kappa estimation, 103 stations with ≥ 4 records were selected, of which 16 stations had *V*s30 values calculated from drilling data and 8 stations had *V*s30 values provided by the Pacific Earthquake Engineering Research Center (PEER) database; the *V*s30 values of the remaining stations were calculated using the following equation (Ghofrani and Atkinson, 2014):

$$\log(Vs30) = 2.76(\pm 0.03) + 0.22(\pm 0.02) \times \log(f_{peak}) - 0.49(\pm 0.05) \times \log(A_{peak}) \quad (1)$$

where f_{peak} and A_{peak} denote the highest peak frequency and peak amplitude, respectively. Equation (1) is valid for $f_{peak} > 1$ Hz, In addition, equation (1) is obtained from the next generation of ground-motion attenuation models for the western United States (NGA-West 2) databases and is usually used for regions with larger peak amplitudes and peak frequencies characterized by shallow soils, such as Japan, China, and Taiwan (Ghofrani and Atkinson, 2014). For H/V curves with peak frequencies less than 1 Hz, we did not calculate the *V*s30 values for these stations, such as stations 53DJL, 51JGD, 51MBQ, and 53DSS. The H/V method is widely used for studying sites where reliable reference sites are lacking or where few observation records are recorded (Zhang et al., 2025), and the H/V curve provide an approximate measure of the amplification of the horizontal component caused by soft layers. At soft-soil sites, the H/V ratio typically exhibits a clear and stable peak, which is associated with the fundamental resonance frequency (Field and Jacob, 1995; Cadet et al., 2012; Pitilakis and Riga, 2013). Therefore, in this study, the peak frequency and corresponding peak amplitude were approximately obtained by the H/V curves.

https://doi.org/10.5194/egusphere-2026-5413
Preprint. Discussion started: 21 September 2026

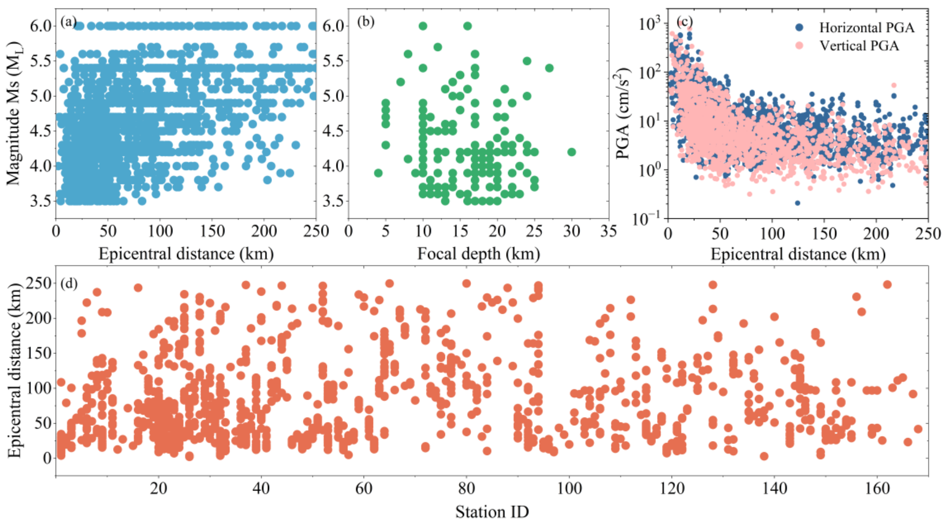

Figure 2. Dataset used for estimating spectral decay parameters. (a) Relationships between earthquake magnitude and epicentral distance, (b) Relationships between magnitude and focal depth, (c) Relationships between PGA and epicentral distance (red for the vertical component and blue for the horizontal component), and (d) epicentral distance ranges of the records at each station.

3. Calculation of the spectral decay kappa

The spectral decay kappa (κ) is defined as the attenuation of the FAS in the high-frequency range greater than a specific frequency (Anderson and Hough, 1984):

$$A(f) = A_0 \exp(-\pi f \kappa),\ f_E < f < f_X \tag{2}$$

where the spectral amplitude A_0 contains the source and path effects, and the frequencies f_E and f_E are the frequencies where the spectral decay starts and ends in log-linear space. In this study, the spectral decay kappa (κ) value was estimated by measuring the slope k of the S-wave FAS on a log-linear scale at high frequencies. The value of f_X–f_E should be greater than 10 Hz to ensure the accuracy of the kappa estimation (Ktenidou et al, 2013). In our scheme, f_E and f_E of each recording were visually picked. Therefore, the slope of the linear portion was obtained by fitting a line to the smoothed FAS curve via the least squares tool. Site effects may significantly affect the kappa estimation. If the fundamental resonance frequency f_0 is well below the frequency range f_X–f_E, kappa estimation will be reliable and unbiased (Parolai and Bindi, 2004). Therefore, in our work, the H/V spectral ratio method was used to select the fundamental resonance frequency of a site, and the frequencies f_E (=1.5f_0) for Class C and Class D sites were determined to be 12 Hz and 9 Hz, respectively. The frequency f_X was manually determined based on the FAS of the S-wave and was basically ranged from 35–50 Hz (Dang et al., 2026).

After the values of parameters f_E and f_X were determined, the high-frequency attenuation kappa (κ) of the acceleration spectrum was calculated via the following equation:

$$\kappa = -k/\pi \tag{3}$$

where k is the slope of the S-wave FAS in linear–log space and can be calculated by $k = \Delta lnA/\Delta f$ (Douglas et al., 2010). In this case, the high-frequency attenuation kappa (κ) from each component for all 165 selected

https://doi.org/10.5194/egusphere-2026-5413
Preprint. Discussion started: 21 September 2026

earthquake events recorded at 103 strong-motion stations in the western-central Sichuan region, China, was estimated. The estimated kappa (κ) values of different earthquake records recorded at the same station are differ because of the influence of the path effect on the kappa values. For this purpose, we used the following equation to estimate the zero-distance κ_0 value related to the site (Anderson and Hough, 1984):

$$\kappa = \kappa_0 + m \times R \tag{4}$$

where κ (s) denotes the kappa value calculated from each component, κ_0 (s) denotes the zero-distance kappa value and may provide information about near-surface attenuation, m (s/km) denotes the fitting coefficient and is related to quality factor and S-wave velocity, and R (km) represents the epicentral distance. The zero-distance κ_0 value is a parameter related to the site that can provide information on near-surface attenuation within several kilometers, and the coefficient m is considered a proxy for regional attenuation and is related to the study region.

4. A site-based kappa model

Spectral decay κ or zero-distance κ_0 is an important parameter in seismology and earthquake engineering, including in stochastic ground motion simulations (Shi and Zhang, 2022; Mao et al., 2024; Dang et al., 2026), adjusting ground motion models for different site conditions (Van Houtte et al., 2011; Biro and Renault, 2012), using the quarter wavelength approach to calculate site amplification (Boore and Joyner, 1997), constraining small-strain damping profiles for site response analysis (Xu et al., 2020; Xu et al., 2021), and investigating kinematic soil-structure interactions (Sotiriadis et al., 2021). In addition, κ_0 and other site parameters, such as Vs30, resonance frequency, and depth-to-bedrock, have always been popular topics (Silva et al., 1998; Edwards et al., 2011; Ktendiou et al., 2015; Altindal and Askan, 2022). In this study, we investigated the factors that affect kappa estimation, such as earthquake size and site conditions, and the sites were simply divided into soft and rock based on the header profiles of the raw acceleration waveforms.

4.1 Investigation of the influencing factors of the kappa value

First, we investigated the impact of different earthquake magnitudes and soil conditions on kappa estimation. We divided the data into three magnitude ranges—3.0–4.0, 4.0–5.0, and 5.0–6.0 and four site condition (soil and rock, Class C and Class D sites). For each set of data, the Shapiro–Wilk test was used to check whether the data followed a normal distribution. The results indicate that the estimated kappa values in each group roughly followed a normal distribution, and Equation (4) was subsequently applied to obtain the kappa model for each group. The kappa values of the EW (0.0013–0.0654 s) and NS (0.0011–0.0738 s) components were generally similar but greater than those of the UD (0.0001–0.0507 s) component. Because m in equation (4) is interpreted as representing regional attenuation, it is region dependent (Edwards *et al.*, 2011). In this study, the kappa models derived from all horizontal and vertical components are $\kappa = 7.20\times10^{-5}R+ (0.0319\pm0.0004)$ and $\kappa = 8.35\times10^{-5}R+ (0.0213\pm0.0006)$, respectively. Accordingly, across all site and event categories, the fitted κ models shared the same slope terms: 7.20×10^{-5} for the EW and NS components, and 8.35×10^{-5} for the UD component.

The intercepts (κ_0) varied as follows: for soil sites, κ_0 was 0.0309 (EW), 0.0325 (NS), and 0.0214 (UD); for rock sites, 0.0330, 0.0333, and 0.0207 (Figure 3a); for Class C sites, 0.0313, 0.0326, and 0.0218; and for Class D sites, 0.0350, 0.0355, and 0.0218 (Figure 3b; Dang et al., 2026). By magnitude, κ_0 values were 0.0296, 0.0321, and 0.0197 for M 3.0–3.9 (Figure 4, top); 0.0313, 0.0326, and 0.0218 for M 4.0–4.9 (Figure 4, middle); and 0.0326, 0.0329, and 0.0219 for M 5.0–6.0 (Figure 4, bottom). All uncertainties are reported as ± standard error. The corresponding zero-distance κ_0 values for each model are shown in Table 1, which indicates that the κ_0

https://doi.org/10.5194/egusphere-2026-5413
Preprint. Discussion started: 21 September 2026

values estimated for the vertical components were significantly smaller than those for the horizontal components and that there was a large difference in κ_0 values between soil sites and rock sites, which differs from the conclusions of Dang et al. (2026), who derived a kappa model based on the same strong-motion data in western-central Sichuan, China, at Class C and Class D sites. In this study, the site conditions given in the raw seismic record header profile were simply used, and Table S1 shows that both the soil and rock sites have Class C and Class D sites, which may be the reasons for the aforementioned false conclusions. However, when the κ_0 values were refit for Class C and Class D sites, the results showed that softer sites have higher κ_0 values, indicating that site conditions significantly affect κ_0 estimates. In addition, as shown in Table 1, the zero-distance κ_0 values depended on the magnitude of the earthquake, with larger magnitudes resulting in larger κ_0 values. This finding is consistent with the conclusions obtained from previous studies (Askan et al., 2014; Neighbors et al., 2015; Perron et al., 2017; Altindal and Askan, 2022; Franceschina and Tento, 2023; Tsurugi et al., 2020). Because the shallow soil layer is horizontally anisotropic, terrain (basin) boundaries can produce direction-dependent amplification and scattering, resulting in different estimated κ_0 values for the two horizontal components. In practical engineering applications, the average of the κ_0 values from the two horizontal components can be used.

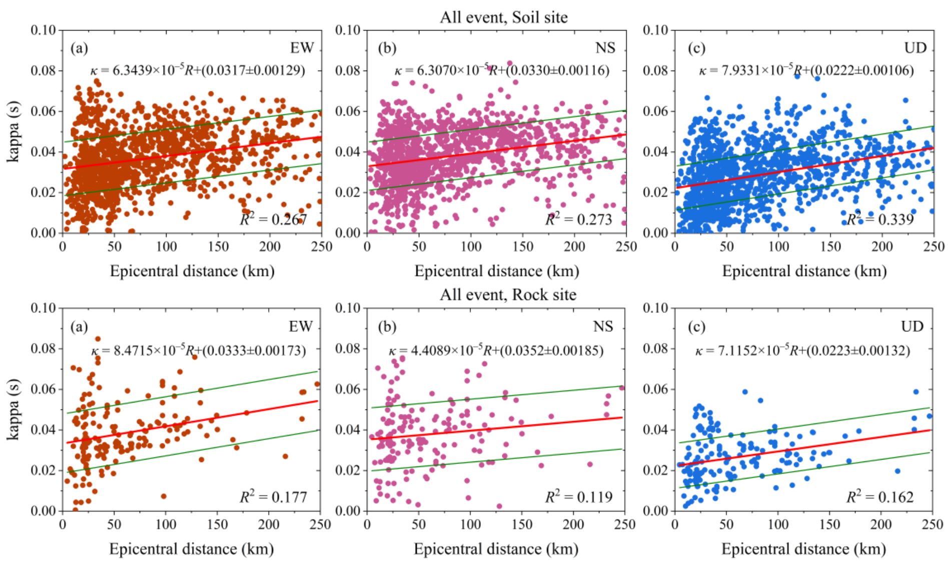

Figure 3. Correlation of the spectral decay kappa values versus the epicentral distance of the EW, NS and UD components for all earthquake events at the soil (top panel) and rock (bottom panel) sites. The red solid line in each panel indicates the results of robust regression, and the green line indicates the $\pm\sigma$ range.

Table 1 Comparison of the zero-distance κ_0 (s) values for different site conditions and magnitude ranges

Site condition and magnitude range		κ_0–EW	SE–EW	p–EW	κ_0–NS	SE–NS	p–NS	κ_0–UD	SE–UD	p–UD
Different site condition (All events)	Soil site	0.0309	0.00168	1.74×10^{-16}	0.0325	0.00183	2.54×10^{-10}	0.0214	0.00119	2.11×10^{-15}
	Rock site	0.0330	0.00500	1.2×10^{-17}	0.0333	0.00498	3.69×10^{-11}	0.0207	0.00298	1.32×10^{-17}
	Class C site	0.0329	0.00338	1.08×10^{-17}	0.0343	0.00365	1.1×10^{-16}	0.0174	0.00175	1.3×10^{-16}

https://doi.org/10.5194/egusphere-2026-5413
Preprint. Discussion started: 21 September 2026

	Class D site	0.0350	0.00345	1.13×10^{-18}	0.0355	0.00371	1.4×10^{-16}	0.0218	0.00239	1.2×10^{-18}
Different magnitude bins	M: 3.0–4.0	0.0296	0.0029	1.2×10^{-17}	0.0321	0.0032	1.1×10^{-17}	0.0197	0.0019	1.3×10^{-19}
	M: 4.0–5.0	0.0313	0.0021	1.01×10^{-18}	0.0326	0.0024	1.1×10^{-16}	0.0218	0.0016	1.4×10^{-17}
	M: 5.0–6.0	0.0326	0.0041	1.21×10^{-18}	0.0329	0.0041	2.2×10^{-16}	0.0219	0.0026	2.7×10^{-16}

Note: SE indicates that the standard error was obtained from the Huber–White sandwich estimator, and the SE value was used to calculate the p value.

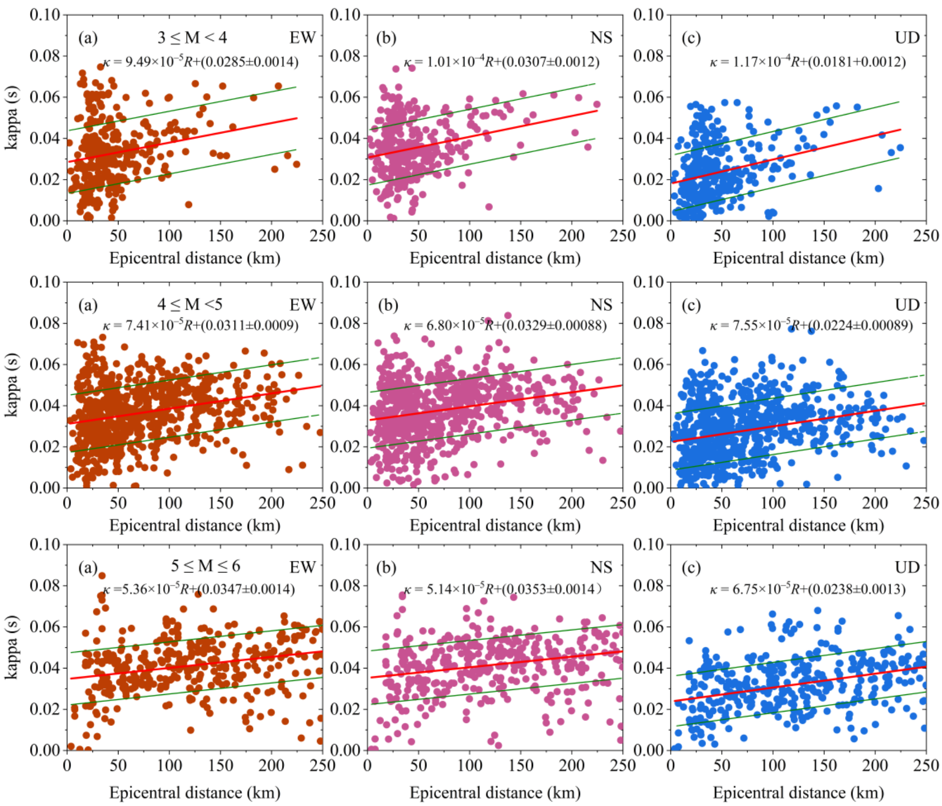

Figure 4. Correlation of the spectral decay kappa values versus the epicentral distance of the EW, NS and UD components. Top panel: earthquake events (3.0≤M<4.0); Middle panel: earthquake events (4.0≤M<5.0); and bottom panel: earthquake events (5.0≤M≤6.0). The red solid line in each panel indicates the results of robust regression, and the green line indicates the $\pm\sigma$ range.

Although κ_0 is generally defined as a site-related parameter, it is closely related to earthquake size. Anderson et al. (1996) reported that zero-distance κ_0 is controlled more by path effects than local site effects, and some studies have indicated that κ_0 is related to magnitude and faulting mechanisms (Tsai and Chen, 2000; Purvance and Anderson, 2003; Biro et al., 2022). However, the results of Kumar et al. (2020) indicated that κ_0 values are not related to source size. Although κ_0 is typically used in earthquake engineering, its physical meaning remains

https://doi.org/10.5194/egusphere-2026-5413
Preprint. Discussion started: 21 September 2026

unclear (Atkinson, 1996; Sun et al., 2013), and it is still unresolved whether it is related to earthquake magnitude. In addition, the Huber–White sandwich estimator was used to calculate the robust standard errors to avoid heteroscedasticity in the standard deviation calculated from the least squares or robust regression, and the small p values ($< 10^{-16}$) obtained from t-test in Table 1 indicate that our results are robust and reliable.

4.2 Station-related κ_0 model and $Vs30$-κ_0 relationships

The zero-distance κ_0 values, which indicate that the near-surface spectral attenuation at the station, depend on the ground characteristics of the station and are specific to each site. The kappa model at each selected station with 4 or more events was derived using robust regression. The resulting station-related κ_0 values for the EW, NS, and UD components are listed in Table S1. Negative κ_0 values were obtained at Stations 51HSS, 53YSZ, 51NXT, 51SMW, and 51LZT, indicating that the amplitude increases with frequency at these sites. This is considered meaningless given the uncertainty of the measurement (Palmer and Atkinson, 2020). In our scheme, a negative κ_0 value is interpreted as near-zero and is therefore set to zero (Palmer and Atkinson, 2020). Additionally, the Huber–White sandwich estimator was employed to compute robust standard errors. The small p values indicate that the station-related κ_0 values are robust and reliable.

The Vs-kappa corrections significantly affect seismic hazard assessments (Biro and Renault, 2013). Many scholars around the word attempt to develop a universal approach by deriving parameterized relationships from preprocessed evaluations, which enables Vs-kappa corrections to be applied to specific ground motion prediction equations (GMPEs) (Cotton et al., 2006). It can also provide constraints for damping parameters (Xu et al., 2020; Pozo et al., 2023). In this study, we treated $Vs30$ obtained by different methods, such as empirical equations (Group 1), drilling data (Group 2), and the PEER database (Group 3), as a dataset and calculated the relationship between κ_0 and $Vs30$ of the horizontal and vertical ground motion components. The robust regression method yields the following relationships:

$$\kappa_{0-H} = (0.0510 \pm 0.0568) - 0.00298 \ln(V_s30) \quad (5)$$

$$\kappa_{0-V} = (0.0206 \pm 0.0591) - 0.00128 \ln(V_s30) \quad (6)$$

in which function ln(*) indicates the natural logarithm of the number *. The correlation coefficients for the above two relationships are 0.124 and 0.164, respectively. To eliminate errors caused by different methods of obtaining $Vs30$ parameters, we conducted a statistical analysis on the Vs-kappa relationship of three sets of data (empirical equation, drilling data, and PEER database), and the results are shown in Figure S2, which indicates that the relationships of these three sets of data are defined as follows: κ_0-H = (0.0450 ± 0.1911) –0.00169ln($Vs30$) and κ_0-V = (0.0654 ± 0.2158) –0.00687ln($Vs30$) for Group 1, κ_0-H = (0.1612 ± 0.1405) –0.022ln($Vs30$) and κ_0-V = (0.2535 ± 0.1779–0.0402ln($Vs30$) for Group 2, and κ_0-H = (0.11834 ± 0.09542) –0.01352ln($Vs30$) and κ_0-V = (0.0326 ± 0.1147) –0.00234ln($Vs30$) for Group 3. Group 1 has a very weak correlation because of the possibility of significant errors in the estimation of $Vs30$ using Equation (1), which may not be suitable for western-central Sichuan, China. For example, from Table S2 in the supplemental material of Dang et al. (2026), the $Vs30$ of Sation 51YAS obtained from the drilling data is 395.98 m/s, whereas the estimated value from Equation (1) is 607.72 m/s, and the $Vs30$ of Station 51SMW calculated from the drilling data is 296.15 m/s, whereas Equation (1) yields 440.0 m/s. The $Vs30$-κ_0 relationships for Groups 2 and 3 are similar, whereas the relationship for Group 1 differs markedly. Similar to the pattern of the $Vs30$-κ_0 correlation obtained from the three groups of data

https://doi.org/10.5194/egusphere-2026-5413
Preprint. Discussion started: 21 September 2026

in this study, most scholars have also derived a negative $Vs30$-κ_0 correlation (Nye et al., 2022). In general, inaccurate $Vs30$ values and limited strong motions tend to contribute to poor $Vs30$-κ_0 relationships.

The relationships between zero-distance κ_0 and the fundamental frequency of site f_0 obtained from earthquake events for stations with 10 or more events (top panel) and stations with 4 or more events (bottom panel) are shown in Figure 5. The results showed that the EW and UD components yielded an expected model and that our derived κ_0-f_0 correlations were consistent with the model given by Pozo et al. (2023), the results show that a larger κ_0 value results in a smaller f_0 value, which indicates that although κ_0 has strong regional characteristics, the κ_0-f_0 correlations is independent of the region. In addition, the estimated $\log\kappa_0$-$\log f_0$ correlation for sites with more records is more reliable. However, the EW component exhibited a slightly weak positive relationship, which was not statistically significant. Interestingly, compared with the $\ln Vs30$-κ_0 correlation, the $\log\kappa_0$-$\log f_0$ correlation seems to be more reliable, as its R^2 value is greater than the R^2 value obtained from the $Vs30$-κ_0 correlation using drilling data and the PEER data. Notably, a significant effect of regional site conditions on the κ_0-f_0 correlations was observed.

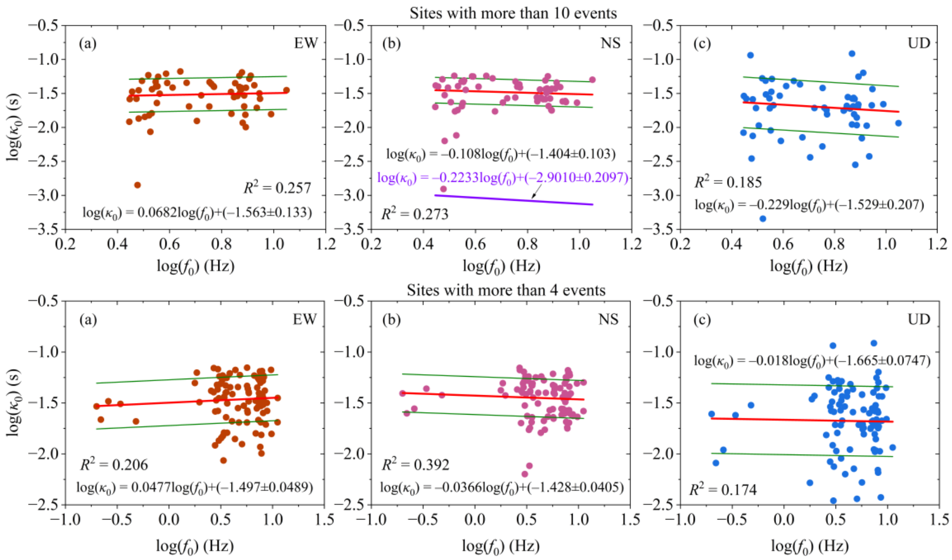

Figure 5. Relationships between zero-distance κ_0 and the fundamental frequency of site f_0 obtained from earthquake events for stations with more than 10 events (top panel) and stations with more than 4 events (bottom panel). The red and green solid lines represent the fitted model and $\pm\sigma$ range, respectively. The R^2 values are also shown in the figure. The purple line in the second panel represents the model derived by Pozo et al. (2023).

5. Stochastic ground motion simulation

The spectral decay kappa parameter is known to be among the key model parameters in the stochastic ground motion simulation technique (EXSIM). To validate the derived site-based kappa model in this study, we performed ground motion simulations of selected earthquake recordings at varying distances. In our simulation, the stochastic finite-fault model was used. In this model, the large rupture fault was consistently subdivided into

https://doi.org/10.5194/egusphere-2026-5413
Preprint. Discussion started: 21 September 2026

smaller subfaults, and each subfault could be considered a point source. In this case, the FAS in the frequency domain was obtained as the product of the source, site and path items. The rupture propagated radially from the initiation point at a given rupture velocity and then caused other subfaults to rupture in turn. The stochastic point-source model was used to estimate the acceleration time history of subfaults, and then the acceleration waveform, $a(t)$, generated by a large fault was composed of the acceleration time histories (a_{ij}) of all subfaults stacked with a certain time delay:

$$a(t) = \sum_{i=1}^{n} \sum_{j=1}^{m} a_{ij}(t + \Delta t_{ij}) \tag{7}$$

where n and m are the numbers of subfaults along the strike and dip of the large fault. Δt_{ij} represents the relative time delay at which the waves from the ijth subfault arrive at the station.

The model parameters that need to be input into the EXSIM algorithm include source, path and site parameters. The source model used in this simulation was given by Guo et al. (2022), which indicates that the moment magnitude of the Changning, China, earthquake is 5.7, and the maximum slip is approximately 0.25 m. The path effect is defined as the product of a trilinear geometrical spreading function and a frequency-related quality factor for central-western China, $Q(f) = 327.8 f^{0.591}$ as derived by Dang et al. (2023). In addition, the four-segment path duration proposed by Atkinson and Boore (1995) is adopted in EXSIM. The stress drop is set to 8 MPa using a trial-and error tool, which controls the amplitude level of the high-frequency spectrum, and the rise time was defined as $1/f_0$ (Boore, 2003), where f_0 denotes the corner frequency. To compare the impact of κ_0 on the simulation results, we estimated the event-related κ_0 based on the Changning, China, earthquake records, as shown in Figure S3. The kappa models for the EW and NS components were as follows: $\kappa = 7.20\times10^{-5}R+(0.0266\pm0.0030)$ and $\kappa = 7.20\times10^{-5}R+(0.0293\pm0.0033)$; the corresponding zero-distance κ_0 values were 0.0266 and 0.0293, respectively, and finally, an average value of 0.027 was used. If the site is classified as a soft soil site, both crustal amplification and local site amplification factors should be considered in EXSIM (Yalcinkaya et al., 2012). Owing to the lack of detailed local site conditions, the H/V spectral ratio approach was used to roughly estimate the local site amplification factor at each station and the crustal amplifications for NEHRP Class C and D sites were given by Boore and Joyner (1997) (Figure S4). Although the crustal amplification factors were derived from North America data, they are widely applied in strong ground motion simulations in other regions (Ma and Xie, 2026). The zero-distance kappa value at each station was derived in this study. The other input parameters can be found in Table S2.

The simulated 5%-damped pseudospectra acceleration (PSA), FAS, and peak ground acceleration (PGA) values were then obtained from EXSIM. In addition, the event-related κ_0 was also used to estimate the above simulated values. In this simulation, all the simulated values (PSA and FAS) were the average of 30 simulations, whereas the PGA values were obtained from the acceleration time history, with its PGA closest to the average of 30 simulations. The observed PSAs were compared with the synthesized PSAs in Figure 6, where the blue solid lines indicate the observed PSAs, and the green and orange solid lines indicate the simulated PSA. At most stations, the simulated and observed PSA values were highly consistent, such as those at stations 51GXT and 53YJT. However, at stations 53DJL, 53DSS, 51LBH, 51LZT, 51MCX, 51YBY, and 51ZG2, significant differences were observed between the simulated and observed values in a short period of 0.1–0.2 s.

https://doi.org/10.5194/egusphere-2026-5413
Preprint. Discussion started: 21 September 2026

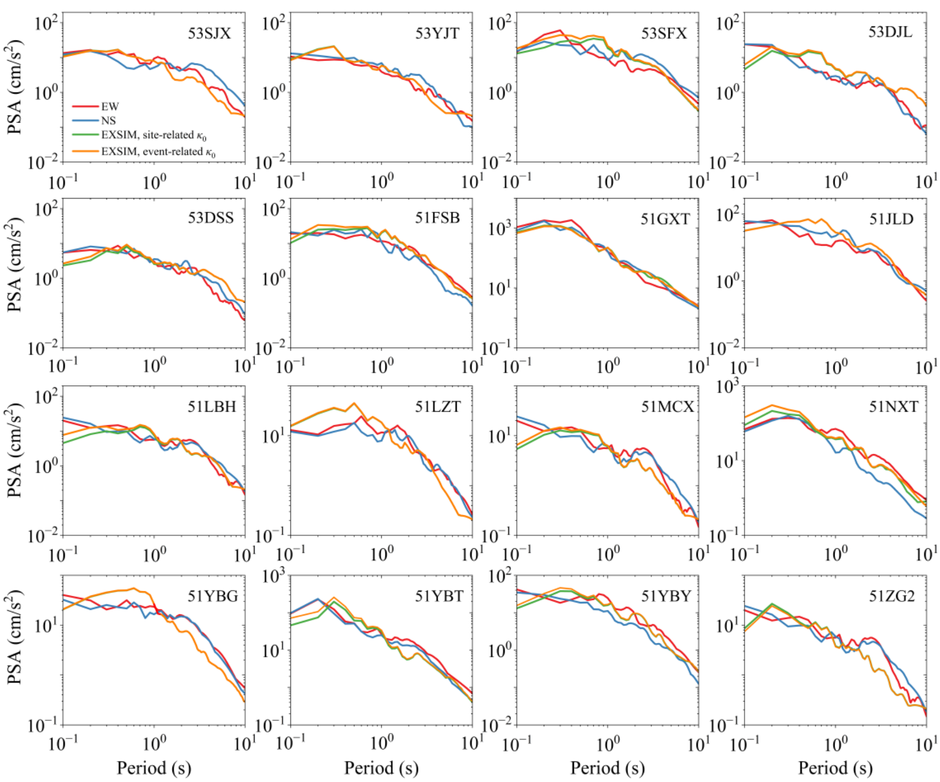

Figure 6. Comparison between simulated and observed PSA values at 16 selected ground motion stations. Red and blue solid lines indicate the PSAs obtained from the EW and NS components, respectively, and the green and orange solid lines represent the simulated PSAs obtained from site-related κ_0 and event-related κ_0, respectively.

For the FAS (shown in Figure S5), the simulated FAS values obtained from event-related and event-related κ_0 values exhibit significant differences primarily at high frequencies, yet both were well matched with the observed values, such as at stations 53YJT, 53SFX, 51FSB, 51JLD, 51LBH, 51LZT, 51MCX, 51NXT, 51YBG, 51YBY, and 51ZG2, whereas at station 53DSS and 51GXT, the simulated values obtained from the two kappa models were consistent with the observed values. However, at stations 53SJX, 53YJT, 53SFX, 51FSB, 51JLD, 51LBH, 51YBY, and 51MCX, the simulation results obtained from both site-related and event-related κ_0 values at low frequencies differed significantly from the observed FAS values, which may be resulted from the complexity of the seismic source and near-surface site amplification. In general, the rupture fault plane of a large earthquake event is very complex, and consists of many parts of different sizes; in EXSIM, the fault plane is simply regarded as a rectangle. The finite-fault joint inversion results of the Changning earthquake indicate that the ruptured fault is composed of a low-angle fault segment F1 and a vertical fault segment F2 (Guo et al., 2022).
Overall, the κ_0 value exhibited a significant effect on the high-frequency simulation results, and the simulation results were highly sensitive to the κ_0 values, which is consistent with the conclusion given by Sun et al. (2013).

https://doi.org/10.5194/egusphere-2026-5413
Preprint. Discussion started: 21 September 2026

In addition, the simulated PGAs obtained from site-related κ_0 values are listed in Table S3, and comparisons with the observed values revealed that at most selected stations, the difference between the simulated values and observed values was small.

Finally, the model bias is defined as log(Simulated value/Observed value) (log(Sim./Obs.)) over all the periods ranging from 0.1 s to 10 s. The model biases obtained from site-related and event-related κ_0 models are shown in Figure 7. As seen in this figure, the model biases calculated by both κ_0 models were between –0.30 and 0.30, and the bias obtained from site-related κ_0 was relatively smaller than that obtained from event-related κ_0 in short periods ($T < 1.0$ s). This indicates that the effect of zero-distance κ_0 on the simulation results is mainly manifested in short periods, while in the long period, the difference in the ground motions synthesized by event-related κ_0 and site-related κ_0 is very small. This is consistent with the results of Dang et al. (2022). In addition, the t-test was used to test whether there was a significant difference between the residual mean and the test mean of 0 (null hypothesis $H_0 = 0$). The test results revealed that at a confidence level of $\alpha = 0.05$, the 95% confidence intervals estimated by the site-related κ_0 model and the event-related κ_0 model were [–0.02762, 6.1128×10^{-4}] and [–0.01799, 0.01134], respectively, with p values of 0.071 and 0.654, respectively. This indicates that the model residuals calculated in this study are not significantly different from zero in the long-period range, thus verifying the reliability of our simulation results.

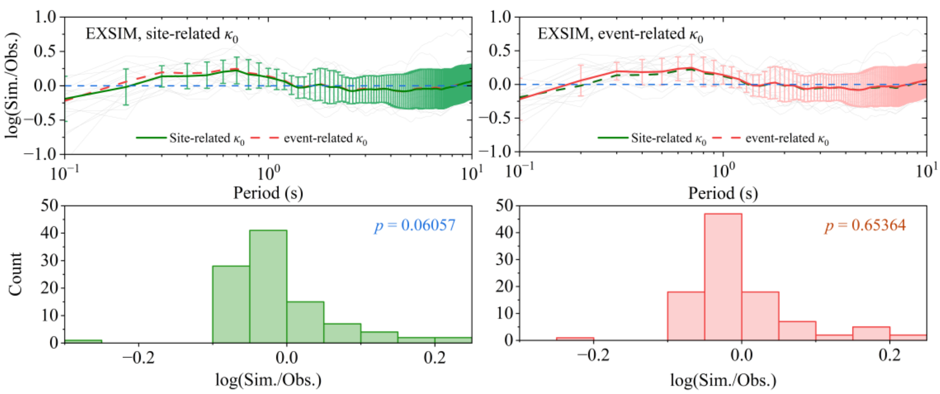

Figure 7. Model bias of the EXSIM simulation results. Top panel: bias defined as the logarithmic value of the ratio between the simulated and observed PSAs across all the selected stations. The grey thin solid line represents the bias at each station, the green and red thick solid lines represent the mean bias, and the green and red thin solid lines represent ±1 standard deviation. Bottom panel: t-test results of the bias.

6. Conclusions

A total of 4260 ground-motion recordings of 165 earthquake events with magnitudes of 3.0–6.0 recorded by 168 stations in western-central Sichuan, China, were collected to derive a spectral decay kappa model and the Vs30-κ_0 relationship in this study. In addition, we investigated the influence of source size and site conditions on the spectral attenuation kappa parameter. The Vs30-κ_0 relationship corresponding to Vs30 estimated by the drilling data, the PEER database, and the empirical equation was derived separately. The spectral decay kappa parameter is known to be among the key model parameters in the EXSIM method. To validate the site-based kappa model

https://doi.org/10.5194/egusphere-2026-5413
Preprint. Discussion started: 21 September 2026

derived in this study, the acceleration waveforms of 16 selected stations triggered by the Changning earthquake were simulated using event-related and site-related κ_0 values, and the influence of these two sets of κ_0 models on the ground motion simulation results was investigated. The main conclusions of this study are as follows:

1. We investigated the impact of different earthquake magnitudes and soil conditions on kappa estimation and reported that the κ_0 values estimated for the vertical components are significantly smaller than those for the horizontal components and that there is a large difference in κ_0 values between soil sites and rock sites. In addition, the results showed that the zero-distance κ_0 values depend on the magnitude of the earthquake, with larger magnitudes resulting in larger κ_0 values.

2. The Vs-kappa corrections significantly affect the seismic hazard assessments. In this study, we treated Vs30 obtained by different methods, such as empirical equation (Group 1), drilling data (Group 2), and the PEER database (Group 3), and the corresponding relationships were derived. The results show that Group 1 has a very weak correlation because of the possibility of significant errors in the estimation of Vs30, whereas there is no significant difference in the Vs30-κ_0 relationships obtained from Groups 2 and 3. In general, a negative Vs30-κ_0 correlation was derived, this is largely due to the fact that there are fewer records for the station, leading to an inaccurate estimation of the station's kappa value. Inaccurate Vs30 values and limited strong motions tend to contribute to poor Vs30-κ_0 relationships. Therefore, the relationships obtained from the sites with 10 or more events are more reliable. In addition, from the statistical parameters, the logκ_0-logf_0 correlation appears to be more reliable compared with the ln$V$s30-κ_0 correlation. A more stable relationships requires more records, and the influence of magnitude and site conditions on the relationship should be considered.

3. To validate the derived site-based kappa model in this study, we performed ground motion simulations of selected earthquake recordings at varying distances. The results show that the κ_0 value is associated with amplitude levels in the short periods range, and the simulation results obtained from both site-related and event-related κ_0 values at low frequencies ($f < 1$ Hz) differ significantly from the observed FAS values. The model biases calculated by both κ_0 models are between –0.30 and 0.25, and the model bias obtained from site-related κ_0 is smaller than that obtained from event-related κ_0. In addition, the model bias and t-test results verified that our simulation results in the long-period range are reliable.

Data Availability

The EXSIM code is available at http://daveboore.com www.daveboore.com/software_online.html (last accessed August 2018). Acceleration waveforms were provided by the China Strong Motion Network Centre (https://data.earthquake.cn/datashare/report.shtml?PAGEID=datasourcelist&dt=40280d0453e5add30153e5e79dc6001b (last accessed December 2022) upon reasonable request (csmnc@iem.ac.cn). Data supporting the fundings of this study are available from the Institute of Engineering Mechanics, China Earthquake Administration upon reasonable request. Earthquake parameters (hypocentre locations, Ms, and M_L) were obtained from the China Earthquake Network Center (https://news.ceic.ac.cn/, last accessed May 2023). Figures were produced using Generic Mapping Tools (GMT) version 5.2.1 (https://www.gmt-china.org/#download, last accessed May 2018) and Origin software (https://www.originlab.com/, last accessed May 2018). The Ms–M_L conversion relationship is available at https://blog.sciencenet.cn/blog-575926-686661.html (last accessed August 2023).

Financial support

This research was supported by the National Natural Science Foundation of China (No. 42204050), the Exploration Project of Zhejiang Natural Science Foundation (Grant No. 422600573), and an Enterprise-Commissioned Science and Technology Project (Grant No. HX2026000339).

Acknowledgements

The authors are thankful to the China Strong Ground Motion Networks Center for providing the strong ground motion data and the American Journal Experts for providing the linguistic assistance during the preparation of the original and revised manuscript. Moreover, we are also thankful to anonymous reviewers and the editors related for their meticulous editing and critical comments that improved the manuscript.

Author contributions

PD was responsible for the study conception and design. Material preparation and data collection were conducted by PD and BZ. All figures were made by PD, and the data analysis was performed by PD, BZ, QL, and JC. The original draft and subsequent revisions of the manuscript were written by PD. All authors reviewed and commented on earlier drafts and approved the final manuscript.

Competing interests

The authors acknowledge that there are no conflicts of interest recorded.

References

Altindal, A., and Askan, A.: Predictive kappa (κ) models for Turkey: Regional effects and uncertainty analysis, Earthquake Spectra, 38(4), 2479-2499, 2022.

Anderson, J. G.: A preliminary descriptive model for the distance dependence of the spectral decay parameter in southern California, Bulletin of the Seismological Society of America, 81(6), 2186-2193, 1991.

Anderson, J. G., and Hough, S. E.: A model for the shape of the Fourier amplitude of acceleration at high frequencies, Bulletin of the Seismological Society of America, 74(5), 1969-1993, 1984.

Anderson, J. G., Lee, Y., Zeng, Y., and Day, S.: Control of strong motion by the upper 30 meters, Bulletin of the Seismological Society of America, 86,1749-1759, 1996.

Askan, A., Sisman, F. N., and Pekcan, O.: A regional near-surface high frequency spectral attenuation (kappa) model for northwestern Turkey, Soil Dynamics and Earthquake Engineering, 65, 113-125, 2014.

Atkinson, G. M.: The high-frequency shape of the source spectrum for earthquakes in eastern and western Canada, Bulletin of the Seismological Society of America, 86, 106-112, 1996.

Atkinson, G. M., and Boore, D. M.: Ground-motion relations for eastern north America, Bulletin of the Seismological Society of America, 85(1), 17-30, 1995.

Biro, Y., and Renault, P.: Importance and impact of host-to-target conversions for ground motion prediction equations in PSHA, 15th word conference of earthquake engineering, Lisboa, 24-28 September, 2012.

Biro, Y., and Renault, P.: A parameterized relation for Vs-Kappa corrections to adjust the global ground motion prediction equations to Swiss NPP sites, 22th Conference on Structural Mechanics in Reactor Technology., San Francisco, California, USA-August 18-23, 2013.

Biro, Y., Siyahi, B., and Akbas, B.: Spectral decay parameter (κ) analysis for a single fault source and an automatic selection procedure for spectral flattening frequency (f_x), Soil Dynamics and Earthquake Engineering, 153, 107122, 2022.

https://doi.org/10.5194/egusphere-2026-5413
Preprint. Discussion started: 21 September 2026

Boore, D. M.: Simulation of ground motion using the stochastic method, Pure and Applied Geophysics, 160(3-4), 635-676, 2003.

Boore, D. M., and Joyner, W. B.: Site amplifications for generic rock sites, Bulletin of the Seismological Society of America, 87(2), 327-341, 1997.

Bora, S. S., Scherbaum, F., Kuehn, N., Stafford, P., and Edwards, B.: Development of a response spectral ground-motion prediction equation (GMPE) for seismic-hazard analysis from empirical fourier spectral and duration models, Bulletin of the Seismological Society of America, 105, 2192-2218, 2015.

Cadet, H., Bard, P. Y., Duval, A. M., and Bertrand, E.: Site effect assessment using KiK-net data: part 2-site amplification prediction equation based on f_0 and V_{SZ}, Bulletin of Earthquake Engineering, 10, 451-489, 2012.

Campbell, K.W.: Estimation of shear-wave Q and κ_0 for unconsolidated and semi-consolidated sediments in Eastern North America, Bulletin of the Seismological Society of America, 99, 2365-2392, 2009.

Castro, R. R., Trojani, L., Monachesi, G., Mucciarelli, M., and Cattaneo, M.: The spectral decay parameter κ in the region of Umbria-Marche, Italy, Journal of Geophysical Research, 105, 23811-23823, 2000.

Cotton, F., Scherbaum, F., Bommer, J. J., and Bungum, H.: Criteria for selecting and adjusting ground-motion models for specific target regions: application to Central Europe and rock sites, Journal of Seismology, 10, 137-156, 2006.

Dabaghim, M., and Kiureghian, A. D.: Stochastic model for simulation of near-fault ground motions, Earthquake Engineering & Structural Dynamics, 46(6), 963-984, 2016.

Dang, P. F., Cui, J., and Liu, Q. F.: Parameter estimation for predicting near-fault strong ground motion and its application to Lushan earthquake in China, Soil Dynamics and Earthquake Engineering, 156, 107223, 2022.

Dang, P. F., Cui, J., and Liu, Q. F.: Research progress on input parameter models for stochastic finite fault ground motion simulation, China Earthquake Engineering, 48(1), 145-156, 2026. (in Chinese)

Dang, P. F., Cui, J., Yang, H. F., and Song, J.: Regional spectral characteristics, quality factor and site responses in western-central Sichuan, China (I): Application of parametric generalized inversion technique, Soil Dynamics and Earthquake Engineering, 176, 108303, 2024.

Dang, P. F., Cui, J., Yang, H. F., and Song, J.: Estimation of source characteristics, site effects and path attenuation in the Sichuan Basin, China, using a non-parametric generalized inversion technique, Geophysical Journal International, 240(2), 1028-1047, 2025.

Dang, P. F., Cui, J., Zhao, B. Y., and Liu, Q. F.: Near-surface high-frequency spectral decay kappa (κ) model of S waves in western-central Sichuan, China, Seismological Research Letters, 97(3), 1946-1964, 2026.

Dang, P. F., Yang, H. F., Cui, J., and Song, J.: Regional spectral characteristics, quality factor and site responses in western-central Sichuan, China (II): Application to stochastic ground motion simulation, Soil Dynamics and Earthquake Engineering, 175, 108274, 2023.

Douglas, J., Gehl, P., Bonilla, L. F., and Gelis, C.: A κ model for mainland France, Pure and Applied Geophysics, 167, 1303-1315, 2010.

Drouet, S., and Chevrot, S.: Simultaneous inversion of source spectra, attenuation parameters, and site responses: application to the data of French Accelerometric Network, Bulletin of the Seismological Society of America, 98, 198-219, 2008.

https://doi.org/10.5194/egusphere-2026-5413
Preprint. Discussion started: 21 September 2026

Edwards, B., Fäh, D., and Giardini, D.: Attenuation of seismic shear wave energy in Switzerland, Geophysical Journal International, 185(2), 967-984, 2011.

Field, E. H., and Jacob, K. H.: A comparison and test of various site-response estimation techniques, including three that are not reference site dependent, Bulletin of Earthquake Engineering, 85, 1127-1143, 1995.

Franceschina, G., and Tento, A.: High frequency attenuation of S waves in alluvial deposits of the central Po Plain (northern Italy), Geophysical Journal International, 234, 2075-2094, 2023.

Ghofrani, H., and Atkinson, G. M.: Site condition evaluation using horizontal-to-vertical response spectral ratios of earthquakes in the NGA-West 2 and Japanese databases, Soil Dynamics and Earthquake Engineering, 67, 30-43, 2014.

Guo, X. Y., Zhang, X., Li, D. H., Yi, L., and Luo, J.: Source characteristics of the shallow 2019 Ms 6.0 Changning, China, earthquake sequence in the salt mining area, Seismological Research Letters, 93(5), 2599-2611, 2022.

Hanks, T. C.: f_{max}, Bulletin of the Seismological Society of America, 72, 1867-1879, 1982.

Hassani, B., and Atkinson, G. M.: Referenced empirical ground-motion model for eastern north America, Seismological Research Letters, 86, 477-491, 2015.

Huang, J. Y., Chao, S. H., Lin, C. M., Chou, C. C., Loh, C. H., and Wu, C. L.: Site-specific response spectra developed by considering near-fault motion with finite-fault simulation in Taiwan, Earthquake Engineering & Structural Dynamics, 53, 968-991, 2024.

Husid, P.: Gravity effects on the earthquake response of yielding structures., California Institute of Technology, California, 1967.

Kilb, D., Biasi, G., Anderson, J. G., Brune, J. N., Peng, Z., and Vernon, F. L.: Comparison of spectral parameter kappa from small and moderate earthquakes using southern California ANZA seismic network data, Bulletin of the Seismological Society of America, 102, 284-300, 2012.

Konno, K., and Ohmachi, T.: Ground-motion characteristics estimated from spectral ratio between horizontal and vertical components of microtremor, Bulletin of the Seismological Society of America, 88, 228-241, 1998.

Ktenidou, O. J., Abrahamson, N. A., Drouet, S., and Cotton, F.: Understanding the physics of kappa (κ): Insights from a downhole array, Geophysical Journal International, 203(1), 678-691, 2015.

Ktenidou, O. J., Cotton, F., Abrahamson, N. A., and Anderson, J. G.: Taxonomy of κ: A review of definitions and estimation approaches targeted to applications, Seismological Research Letters, 85(1), 135-146, 2014.

Ktenidou, O. J., Gelis, C., and Bonilla, L. F.: A study on the variability of kappa (κ) in a borehole: implications of the computation process, Bulletin of the Seismological Society of America, 103, 1048-1068, 2013.

Kumar, V., Chopra, S., Choudhury, P., and Kumar, D.: Estimation of near surface attenuation parameter (κ) in Northwest and Northeast Himalaya region, Soil Dynamics and Earthquake Engineering, 136, 106237, 2020.

Laurendeau, A., Cotton, F., Ktenidou, O. J., Bonilla, L. F., and Hollender, F.: Rock and stiff-soil site amplification: dependency on Vs30 and kappa (κ_0), Bulletin of the Seismological Society of America, 101, 2926-2941, 2013.

Mao, L., Shi, Y. C., Lu, Y. X., and Liu, K.: Three-component ground motion simulation for the 2023 Ms6.2 earthquake in Jishishan, Gansu, based on the stochastic finite-fault method, China Earthquake Engineering, 46(4), 778-790, 2024. (in Chinese)

https://doi.org/10.5194/egusphere-2026-5413
Preprint. Discussion started: 21 September 2026

Motazedian, D., and Atkinson, G. M.: Stochastic finite-fault modeling based on a dynamic corner frequency, Bulletin of the Seismological Society of America, 95(3), 995-1010, 2005.

Moya, A. J., Aguirre, J., and Irikura, K.: Inversion of source parameters and site effects from strong ground motion records using genetic algorithms, Bulletin of the Seismological Society of America, 90, 977-992, 2000.

Neighbors, C., Liao, E. J., Cochran, E. S., Funning, G. J., Chung, A. I., Lawrence, J. F., Christensen, C., Miller, M., Belmonte, A., and Sepulveda, H. H. A.: Investigation of the high-frequency attenuation parameter, κ (kappa), from aftershocks of the 2010 Mw8.8 Maule, Chile earthquake, Geophysical Journal International, 200, 200-215, 2015.

Nye, T., Sahakian, V. J., King, E., Baltay, A., and Klimasewski, A.: Estimation of κ_0 and effects on ground motions in the San Francisco Bay area, Bulletin of the Seismological Society of America, 113(2), 823-842, 2022.

Palmer, S. M., and Atkinson, G. M.: The High-Frequency Decay Slope of Spectra (kappa) for M≥Earthquakes on Rock Sites in Eastern and Western Canada, Bulletin of the Seismological Society of America, 110(2), 471-488, 2020.

Papageorgiou, A. S., and Aki, K.: A specific barrier model for the quantitative description of inhomogeneous faulting and the prediction of strong ground motion, Bulletin of the Seismological Society of America, 73, 693-722, 1983.

Parolai, S., and Bindi, D.: Influence of soil-layer properties on κ evaluation, Bulletin of the Seismological Society of America, 94, 349-356, 2004.

Perron, V., Hollender, F., Bard, P. Y., Gelis, C., Guyonnet-Benaize, C., Hernandez, B., and Ktenidou, O. J.: Robustness of kappa (κ) measurement in low-to-moderate seismicity area: Insight from a site-specific study in Provence, France, Bulletin of the Seismological Society of America, 107(5), 256-275, 2017.

Pitilakis, K., Riga, E., and Anastasiadis, A.: New code site classification, amplification factors and normalized response spectra based on a worldwide ground motion database, Bulletin of Earthquake Engineering, 11, 925-966, 2013.

Pozo, I., Montalva, G., and Miller, M.: Assessment of kappa values in the Chilean subduction zone for interface and in-slab events, Seismological Research Letters, 94(1), 385-398, 2023.

Purvance, M. D., and Anderson, J. G.: A comprehensive study of the observed spectral decay in strong-motion accelerations recorded in Guerrero, Mexico, Bulletin of the Seismological Society of America, 93(2), 600-611, 2003.

Rovelli, A., Bonamassa, O., Cocco, M., Bona, M., and Mazza, S.: Scaling laws and spectral parameters of the ground motion in active extensional areas in Italy, Bulletin of the Seismological Society of America, 78(2), 530-560, 1988.

Sertcelik, F., Akcay, D., Livaoglu, H., and Gerdan, S.: The spectral decay parameter kappa in Marmara region, Turkey, Arabian Journal of Geosciences, 15, 271, 2022.

Shi, H. B., and Zhang, Y. S.: Strong ground motion simulation of the Qinghai Ms6.9 earthquake on January 8, 2022, China Earthquake Engineering, 46(3), 680-691, 2024. (in Chinese)

Silva, W., Darragh, R., Gregor, N., Martin, G., Abrahamson, N., and Kircher, C.: Reassessment of site coefficients and near-fault factors for building code provisions, Technical Report Program Element II: 98-HQGR-1010 Pacific Engineering and Analysis, EI Cerrito, USA, 1998.

Sotiriadis, D., Margaris, B., Klimis, N., and Sextos, A.: Implications of high-frequency decay parameter, “κ-kappa,” in the estimation of kinematic soil-structure interaction effect, Soil Dynamics and Earthquake Engineering, 144, 106665, 2021.

Sun, X. D., Tao, X. X., Duan, S. S., and Liu, C.Q.: Kappa (κ) derived from accelerograms recorded in the 2008 Wenchuan mainshock, Sichuan, China, Journal of Asian Earth Sciences, 73, 306-316, 2013.

Tsai, C. -C. P., and Chen, K. C.: A model for the high-cut process of strong-motion accelerations in terms of distance, magnitude, and site condition: An example from the SMART 1 Array, Lotung, Taiwan, Bulletin of the Seismological Society of America, 90(6), 1535-1542, 2000.

Tsurugi, M., Tanaka, R., Kagawa, T., and Irikura, K.: High-frequency spectral decay characteristics of inland crustal earthquakes in Japan: evaluation of the fmax and κ models, Bulletin of the Seismological Society of America, 110, 452-470, 2020.

Van, Houtte. C., Drouet, S., and Cotton, F.: Analysis of the origins of κ (kappa) to compute hard rock to rock adjusting factors for GMPEs, Bulletin of the Seismological Society of America, 101(6), 2926-2941, 2011.

Wang, S. Y., Wang, J., Yu, Y. X., Wu, Q., Gao, A. J. & Gao, M. T.: The empirical relation between M_L and Ms based on bulletin of seismological observations of Chinese stations, Earthquake Research in China, 26, 14-22, 2010. (In Chinese)

Xu, B., and Rathje, E. M.: The effect of soil nonlinearity on high-frequency spectral decay and implications for site response analysis, Earthquake Spectra, 37(2), 686-706, 2021.

Xu, B., Rathje, E. M., Hashash, Y., Stewart, J., Campbell, K., and Silva, W.J.: κ_0 for soil sites: Observations form Kik-net sites and their use in constraining small-strain damping profiles for site responses analysis, Earthquake Spectra, 36(1), 111-137, 2020.

Yalcinkaya, E., Pinar, A., Uskuloglu, O., Tekebas, S., and Firat, B.: Selecting the most suitable rupture model for the stochastic simulation of the 1999 Izmit earthquake and prediction of peak ground motions, Soil Dynamics and Earthquake Engineering, 42, 1-16, 2012.

Zhang, B., Lu, X. J., Rong, M. S., Kong, X. S., Wang, J. X., Yu, Y. X., and Li, X. J.: HVSR f_{peak}-based Vs30 estimation model and its applicability to GMPE in southwest China, Seismological Research Letters, 96(5), 3024-3033, 2025.

Zhang, F., Mavroeidis, G. P., and Wang, J. Q.: Validation of physics-based regional-scale ground-motion simulations of the 2008 Mw 7.9 Wenchuan earthquake for engineering applications, Earthquake Engineering & Structural Dynamics, 51(12), 2975-2999, 2021.

Zuo, K. Z., and Zhao, C.P.: The spatial and temporal distribution of source parameters of earthquakes in Changning area, Sichuan province, Earthquake Research in China, 37(2), 472-482, 2021. (in Chinese)

Ma, W. J., and Xie, Z. N.: An improved stochastic finite-fault simulation method and its application to large magnitude thrust earthquakes, Earthquake Engineering and Engineering Vibration, 25(1), 41-53, 2026.